

# Ion acceleration in an expanding plasma

A. V. Gurevich and A. P. Meshcherkin

*P. N. Lebedev Physics Institute, USSR Academy of Sciences*

(Submitted 25 June 1980)

*Zh. Eksp. Teor. Fiz.* **53**, 1810–1826 (May 1981)

We consider ion acceleration when a tenuous plasma expands in a vacuum. It is shown that the ion acceleration is substantially enhanced for electron distributions that are not Maxwellian and are enriched with fast particles. We investigate wave motions in an expanding plasma. The existence of two greatly differing wave types is indicated—front waves and quasi-self-similar waves. The acceleration of ions in a multicomponent plasma is considered. The results of the theory are compared with the experimental data on the acceleration of ions in a plasma produced by intense laser pulses; it is shown that they are in sufficient agreement.

PACS numbers: 52.25.Fi, 52.50.Jm, 52.35. — g

Rapid acceleration of ions when a tenuous plasma expands freely is one of the interesting features of plasma kinetics. The acceleration has a collective character and is due to energetic transfer of electron momentum to the fast ions.<sup>1</sup> It was observed in experiment both in a laboratory plasma<sup>2–5</sup> and in the ionosphere,<sup>6,7</sup> as well as in a laser spark.<sup>8–11</sup> The accelerated ions reach in the latter case energies 1–2 MeV, and carry away a considerable fraction of the absorbed laser spark. One can expect further increase of the energy density in the short laser pulses to increase the role of the accelerated ions even more.<sup>11</sup>

The purpose of the present study was to investigate those distinguishing features of the motion of an expanding tenuous plasma which influence substantially the ion acceleration process. In §1 the plasma expansion is considered for a non-Maxwellian electron distribution function enriched with fast particles. In §2 we study the wave motions in an expanding plasma. Some of them determine the motion of the ion front, while others produce quasi-self-similar waves that cause oscillations of the energy spectra of the accelerated ions. In §3 we investigate a multicomponent plasma containing ions with different masses  $M$  and charges  $Z$ . In the concluding §4 we compare the results of the theory with the laser-experiment data.

## §1. EXPANSION OF A PLASMA IN A VACUUM IN THE CASE OF NONMAXWELLIAN ELECTRON DISTRIBUTION

The expansion of a tenuous plasma in a vacuum is described by a system of collisionless kinetic equations for the electrons and ions, in conjunction with the Poisson equation for the electric-field potential  $\varphi$ . We consider one-dimensional motion—the plasma expands in the direction from  $x \rightarrow -\infty$  to  $x \rightarrow +\infty$ . We assume also that the electric-field potential  $\varphi$  is a monotonic function of  $x$ . Then the one-dimensional distribution function of the electrons  $f_e$  takes the form<sup>2)</sup>

$$f_e(v, x, t) = f_e(-v, x, t) = f_{e0}(v_0), \quad (1)$$

$$v_0 = (v^2 - 2e\varphi/m)^{1/2}.$$

Here  $f_{e0}(v_0)$  is the electron distribution function, specified in the unperturbed region of the plasma at  $x \rightarrow -\infty$  (it is assumed that the potential  $\varphi \rightarrow 0$  as  $x \rightarrow -\infty$ ). Equation (1) is written under the assumption that the

electric-field potential forms a wave moving with velocities on the order of hydrodynamic  $v_t$ , i.e., much slower than the thermal velocities  $v_T$  of the electrons. Therefore, in first-order approximation in  $v_t/v_T$  the variation of the field with time can be neglected, i.e., we can consider the motion of the electrons in a quasi-static field (1).<sup>3)</sup> In this approximation the electron density at an arbitrary point  $(x, t)$  depends only on the electric-field potential

$$N_e(\varphi) = 2 \int_0^\infty f_{e0}((v^2 - 2e\varphi/m)^{1/2}) dv. \quad (2)$$

In particular, in case of a Maxwellian function  $f_{e0}(v_0)$  we get from (1) and (2) an equilibrium Maxwell-Boltzmann distribution for the electrons.

The ion motion is described by the kinetic equation. It is important, however, as shown in Refs. 1, 15, and 17, that with increasing average ion velocity the ion distribution function narrows down rapidly and becomes needle-like. The thermal scatter of the velocities is therefore of little importance for the motion of accelerated ions. They can be described in the hydrodynamic approximation:

$$\frac{\partial N}{\partial t} + v \frac{\partial N}{\partial x} + N \frac{\partial v}{\partial x} = 0, \quad (3)$$

$$\frac{\partial v}{\partial t} + v \frac{\partial v}{\partial x} + \frac{eZ}{M} \frac{\partial \varphi}{\partial x} = 0.$$

Here  $N$  is the density and  $v$  the average velocity in the  $x$  direction of the ions with charge  $eZ$  and mass  $M$ . The electric field is described by the Poisson equation

$$\frac{\partial^2 \varphi}{\partial x^2} = -4\pi e(N - N_e(\varphi)). \quad (4)$$

Here  $N_e(\varphi)$  is the electron density. Equations (1)–(4) are a closed system describing ion acceleration in an expanding plasma.

If the characteristic spatial scale of the expanding plasma  $R$  is much larger than the Debye radius  $D = (T_e/4\pi e^2 N)^{1/2}$ , then the Poisson Eq. (4) reduces, accurate to small terms of order  $(D/R)^2$ , to the quasi-neutrality equation

$$N = N_e(\varphi). \quad (5)$$

Equations (3) and (5) admit of self-similar solutions.

In particular, in the problem where a half-space filled with a plasma having at the initial instant  $t=0$  a sharp boundary at  $x=0$  expands into a vacuum, we have, changing in (3) to the self-similar variable  $\tau=x/t$  and putting  $N=N(\tau)$  and  $v=v(\tau)$ ,

$$\begin{aligned} (v-\tau)\frac{dN}{d\tau} + N\frac{dv}{d\tau} &= 0, \\ (v-\tau)\frac{dv}{d\tau} + \frac{eZ}{M}\frac{d\varphi}{d\tau} &= 0, \end{aligned} \quad (6)$$

where the function  $\varphi=\varphi(N)$  is defined in accordance with (2) and (5). Changing over to the variable  $\varphi$ , we obtain the general solution of Eqs. (6) in the form

$$v=\tau+s(\varphi); \quad N=N_*(\varphi); \quad s^2(\varphi)=eZN_*(\varphi)/M\frac{dN_*}{d\varphi}, \quad (7)$$

where the dependence of  $\tau$  on  $\varphi$  is determined by the relation

$$-\tau=s(\varphi) + \frac{eZ}{M} \int_0^{\varphi} \frac{d\varphi}{s(\varphi)}. \quad (8)$$

We note that by putting  $N=N(v)$  in (6) we can represent the obtained solution also in the form

$$v=\tau+s(v); \quad s^2 = \left[ N(v) \frac{dN}{dv} \right]^2, \quad (8a)$$

where the function  $N(v)$  is determined from the relation

$$dv = \frac{dN}{N} s(N), \quad s(N) = \left[ \frac{eZN}{M} \frac{dN_*(\varphi(N_*))}{d\varphi} \right]^{1/2},$$

and  $\varphi=\varphi(N_*)$  and  $dN_*/d\varphi$  are determined by the quasineutrality Eq. (5).

In the case of a Maxwellian distribution function of the electrons, the solution (7) and (8) agrees with the previously obtained<sup>1</sup> solution

$$\begin{aligned} v &= \tau + s_0, \quad N = N_0 \exp(-\tau/s_0 - 1), \\ \varphi &= -\frac{T_0}{e} \left( \frac{\tau}{s_0} + 1 \right), \quad s = s_0 = \left( \frac{ZT_0}{M} \right)^{1/2}. \end{aligned} \quad (9)$$

In the case of a two-temperature distribution function (i.e., consisting of two Maxwellian functions with different temperatures  $T_0$  and  $T_h \gg T_0$ ), Eqs. (7) and (8) lead to the results of Wickens *et al.*<sup>18</sup>

In the general case the dependence of  $N$  on  $\tau$  or on  $v$ , according to (7), (8), and (8a), is determined essentially by the form of the function  $N_*(\varphi)$  (2), i.e., in final analysis, by the form of the electron distribution function  $f_e(v_0)$  (1).

Figure 1 shows a plot of  $N(\tau)$  for a Maxwellian, a two-temperature, and a power-law<sup>4</sup> distribution function. It is seen that the presence of fast electrons influences strongly the ion acceleration. Interesting qualitative peculiarities also occur. It follows from (7) and (8) that the dependence of  $\tau$  on  $\varphi$  has a monotonic character if the following condition is satisfied<sup>19,20</sup>

$$\frac{d}{d\varphi} \left( \frac{N_*}{dN_*/d\varphi} \right) = \frac{M}{eZ} \frac{ds^2}{d\varphi} > -2. \quad (10)$$

If condition (10) is violated, however, the function  $\tau(\varphi)$  becomes nonmonotonic, and consequently  $\varphi(\tau)$  is not single valued. The density and velocity profiles

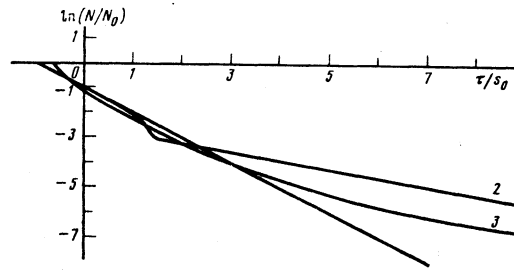


FIG. 1. Ion density  $N$  as a function of  $\tau/s_0$ ,  $s_0 = (T_0/M)^{1/2}$ , for different electron distribution functions: 1—Maxwellian ( $N_0$ ,  $T_0$ ), 2—two-temperature ( $T_h = 9T_0$ ,  $N_h = 0.1N_0$ ), 3—power-law ( $N = N_0/(1-e\varphi/T)^2$ ).

$N(\tau)$  and  $v(\tau)$  contain in this case singular points ( $\partial N/\partial x \rightarrow \infty$ ,  $\partial v/\partial x \rightarrow \infty$ ). These are singular points of hydrodynamic type.<sup>21</sup> In the vicinity of these singular points the quasineutrality condition (5) is violated, and ion-sound oscillations develop. In particular, in the case of a two-temperature distribution function of the electrons the condition (10) is violated if the temperature  $T_h$  of the hot component exceeds by more than 9.6 times the temperature  $T_0$  of the cold electrons.<sup>18</sup>

## §2. WAVES IN AN EXPANDING PLASMA

We have considered above self-similar solutions corresponding to the quasineutral approximation (5). They differ substantially from the exact solutions of the complete system of Eqs. (3) and (4). Indeed, assume that at the initial instant  $t=0$  the ions, just as in the self-similar solution, occupy a half-space and do not move:

$$v_{i=0} = 0, \quad N_{i=0} = \begin{cases} N_0, & x < 0 \\ 0, & x > 0 \end{cases}. \quad (11)$$

In the quasineutral approximation (5) and (2), the initial distribution of the electron density  $N_e$  and of the potential  $\varphi(N_e)$  also takes the form of a jump at  $x=0$ . On the other hand, the exact solution of the Poisson Eq. (4), (11) leads to a different answer:  $N_e$  and  $\varphi$  are smeared out in the vicinity of the boundary  $x=0$ . The solution of Eqs. (4) and (2) is obtained subject to the boundary conditions

$$\begin{aligned} \varphi \rightarrow 0, \quad \frac{\partial \varphi}{\partial x} \rightarrow 0 \quad \text{as} \quad x \rightarrow -\infty \\ \varphi \rightarrow -\infty, \quad \frac{\partial \varphi}{\partial x} \rightarrow 0 \quad \text{as} \quad x \rightarrow +\infty. \end{aligned} \quad (12)$$

The solutions for  $\varphi$  on the right and on the left are joined together at the boundary  $x=0$  (continuity of  $\varphi$  and of  $\partial\varphi/\partial x$ ), where the ion density has a discontinuity. The boundary of the discontinuity or the boundary of the ion front  $x_F(t)$  exists also hereafter at all values of  $t$ . The result of numerical integration of Eqs. (3), (4), and (2) with the initial and boundary conditions (11) and (12) is shown in Fig. 2 for the case of a Maxwellian distribution of the electrons. The dash-dot line in the figure shows the self-similar approximation. It is seen that the exact solution approaches the self-similar solution in the course of time. Its main difference from the self-similar solution is the presence of an abrupt leading front of the ions: at each instant of time  $t$  one can indicate the limiting point  $x_F(t)$  which

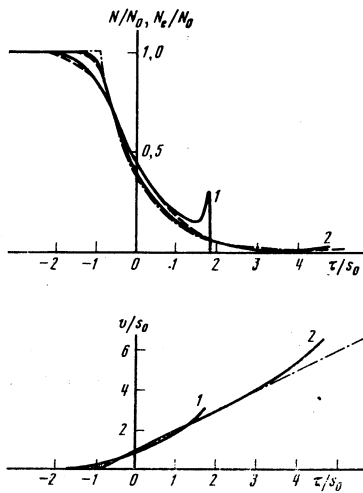


FIG. 2. Densities of the ions  $N$  and of the electrons  $N_e$  (dashed) and the ion velocities  $v_i$  as functions of  $\tau/s_0$  at the instants of time: 1)  $t_1 = 5/\Omega_{0i}$ , 2)  $t_2 = 30/\Omega_{0i} = (4\pi e^2 N_0/M)^{1/2}$ . Dash-dot curve—self-similar solution.

the ions have reached and the limiting velocity  $v_F(t)$  to which the ions were accelerated.

Qualitatively this is easy to understand. The self-similar solution (7)–(9) presupposes, in accord with the very formulation of the problem, that at the initial instant of time  $t=0$  the potential  $\varphi$  near the plasma boundary  $x=0$  changes jumpwise from  $\varphi=0$  (as  $x \rightarrow -0$ ) to  $\varphi=-\infty$  (as  $x \rightarrow +0$ ). The ions are acted upon here, consequently, by an infinite force  $F=e\partial\varphi/\partial x$ . This produces in the plasma immediately ions with arbitrarily large velocities. In the exact solution, the potential  $\varphi(x)$  at  $t=0$  is smeared out, i. e., it varies smoothly. The force acting on the ions is then always finite, so that the ions move with a finite velocity that increases with time. The ions can be accelerated in a finite time only to a fully defined limiting velocity—the velocity of the front  $v_F(t)$ . The ion acceleration depends essentially on the function  $N_e(\varphi)$ , i. e., on the electron distribution function (1). This is seen from Fig. 3,

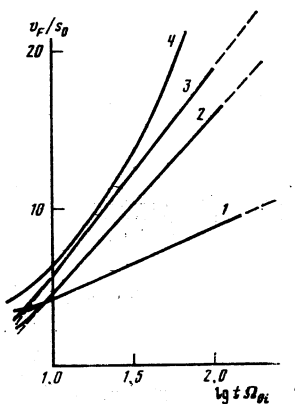


FIG. 3. Ion-front velocity  $v_F/s_0$  as a function of the time  $t$  for different electron distribution functions: 1) Maxwellian ( $N_0, T_e$ ); two-temperature (2— $T_h = 6.67 T_e$ ,  $N_h = 0.02 N_0$ , 3— $T_h = 9 T_e$ ,  $N_h = 0.02 N_0$ ); 4—power law. Dashed—calculation of  $v_F$  by formula (20) for: 1)  $s_0 = (T_e/M)^{1/2}$ , 2, 3)  $s_0 = (T_h/M)^{1/2}$ .

which shows the dependence of the front velocity  $v_F$  on the time for different electron distribution functions. The front velocity increases with increasing number of fast electrons. If the number of fast electrons exceeds (1–2)%, then they practically always determine the velocity of the ion front (see curves 2 and 3 of Fig. 3).

The singularities of the motion of the ion front can be easily understood by considering the behavior of the perturbations in a self-similarly expanding plasma. We seek the solution of Eqs. (3) and (4) in the form

$$N=N_e(\tau)+\delta N(x,t); \quad v=v_e(\tau)+\delta v(x,t); \quad \varphi=\varphi_e(\tau)+\delta\varphi(x,t). \quad (13)$$

Substituting the expansion (13) in Eqs. (3) and (4) and linearizing them, we get

$$\begin{aligned} \frac{\partial\delta N}{\partial t}+v_e\frac{\partial\delta N}{\partial x}+N_e\frac{\partial\delta v}{\partial x}+\frac{1}{t}\left[\delta v\frac{dN_e}{d\tau}+\delta N\frac{dN_e}{d\tau}\right]&=0, \\ \frac{\partial\delta v}{\partial t}+v_e\frac{\partial\delta v}{\partial x}+\frac{eZ}{M}\frac{\partial\delta\varphi}{\partial x}+\frac{1}{t}\delta v\frac{dv_e}{d\tau}&=0, \\ \frac{1}{t^2}\frac{d^2\varphi_e}{d\tau^2}+\frac{\partial^2\delta\varphi}{\partial x^2}&=-4\pi e\left[\delta N-\delta\varphi\left(\frac{dN_e}{d\varphi}\right)\right]. \end{aligned} \quad (14)$$

Considering perturbations whose spatial dimension  $k^{-1}$  is small compared with the characteristic scalar variation of the self-similar solution, but large compared with the Debye radius,

$$(kD)^2 \ll 1 \ll kts, \quad (15)$$

we obtain in place of (14) the wave equation

$$\begin{aligned} \frac{\partial\delta N}{\partial t}+v_e\frac{\partial\delta N}{\partial x}+N_e\frac{\partial\delta v}{\partial x}&=0, \\ \frac{\partial\delta v}{\partial t}+v_e\frac{\partial\delta v}{\partial x}+\frac{eZ}{M(\partial N_e/\partial\varphi)_e}\frac{\partial\delta N}{\partial x}&=0. \end{aligned} \quad (16)$$

Its approximate solution under the conditions (15) is

$$\begin{aligned} \delta N=\delta N_0(x-Vt), \quad \delta v=\delta v_0(x-Vt), \\ V=v_e \pm s, \quad s^2=\frac{eZ}{M}\frac{N_e}{(dN_e/d\varphi)_e}=\left[N_e\left/\frac{dN_e}{d\varphi}\right.\right]^{\frac{1}{2}}. \end{aligned} \quad (17)$$

The result is quite natural—the ions move with velocity  $v_a(\tau)$ , while the perturbations propagate with the speed of sound  $s$  relative to the ions.

The wave traveling towards the rarefaction, which we shall call the wave of the front, has a local velocity

$$v_F=v_e(\tau)+s=\tau+2s(\tau). \quad (18)$$

We have taken into account here expression (7) for the velocity  $v_a(\tau)$ . Since

$$v_F=dx_F/dt=\tau+td\tau/dt,$$

it follows from (18) that

$$\int_{x_F}^{x_F''} \frac{d\tau}{s(\tau)}=2 \ln t. \quad (19)$$

In particular, in the case of Maxwellian electrons (9) we have

$$\begin{aligned} x_F=2ts_0 \ln t+Cts_0, \quad v_F=\frac{dx_F}{dt}=2\left(\frac{ZT_e}{M}\right)^{1/2} \ln(t\Omega_{0i}C_0), \\ \Omega_{0i}=(4\pi e^2 N_0/M)^{1/2}. \end{aligned} \quad (20)$$

The velocity of the wave of the front (20) increases logarithmically with time. It is shown dashed in Fig. 3.

One can see the good agreement with the result of the numerical calculation. The integration constant  $C_0$ , determined by matching to the numerical solution, equals 0.9.

For the front velocity in the case of a two-temperature distribution function, formula (20) is also valid, but the electron temperature  $T_e$  must be replaced by the temperature  $T_h$  of the fast component. The constant  $C_0$  depends in this case on the relative density of the fast particles.

It follows from (19) that the time variation of the ion-front velocity is determined in the general case by the local speed of sound  $s(\tau)$ , which depends substantially on the form of the electron distribution function (5), (7), (8).

We consider now perturbations that move towards the dense plasma. In an immobile coordinate frame they have a velocity (17), (7)

$$V = v_e - s = \tau, \quad (21)$$

i.e., they are self-similar. But strictly-self similar waves are impossible in hydrodynamics, since the self-similar solution (7), (8) is uniquely defined. Perturbations moving towards the dense plasma must therefore be investigated in greater detail, with allowance for the nonlinear and dispersion corrections.

To this end we rewrite the Poisson Eq. (4) in the form

$$\varphi = \varphi_e \left( N + \frac{1}{4\pi e} \frac{\partial^2 \varphi}{\partial x^2} \right). \quad (22)$$

Here  $\varphi_e(N)$  is a specified function, the inverse of the function  $N_e(\varphi)$ , and is defined by the quasineutrality Eq. (5). In the case of a Maxwellian distribution

$$\varphi_e(N) = \frac{T_e}{e} \ln \frac{N}{N_0}. \quad (23)$$

Assuming now that the dispersion and the nonlinear corrections are small, we get from (22)

$$\varphi = \varphi_e(N) + \frac{1}{4\pi e} \frac{d\varphi_e}{dN} \frac{\partial^2 \varphi_e(N)}{\partial x^2} \approx \varphi_e(N) + \frac{1}{4\pi e} \left( \frac{d\varphi_e}{dN} \right)^2 \frac{\partial^2 N}{\partial x^2}.$$

Substituting this expression in (3), we arrive at the equations

$$\begin{aligned} \frac{\partial N}{\partial t} + v \frac{\partial N}{\partial x} + N \frac{\partial v}{\partial x} &= 0, \\ \frac{\partial v}{\partial t} + v \frac{\partial v}{\partial x} + \frac{eZ}{M} \frac{d\varphi_e}{dN} \frac{\partial N}{\partial x} + \frac{Z}{4\pi M} \left( \frac{d\varphi_e}{dN} \right)^2 \frac{\partial^2 N}{\partial x^2} &= 0, \end{aligned} \quad (24)$$

which describe the hydrodynamics of the ions in a plasma with arbitrary distribution of electron velocities and with account taken of the dispersion corrections. In the case of Maxwellian electrons (23), Eqs. (24) coincide with the previously known ones.<sup>22</sup>

When considering waves that are close to self-similar, it is natural to change over from  $x$  and  $t$  to new variables  $\tau$  and  $\xi$ . Separating, in addition, the principal self-similar flow  $\bar{N}_e(\tau), v_e(\tau)$ :

$$N = \bar{N}_e(\tau) + N_1(\tau, \xi), \quad v = v_e(\tau) + v_1(\tau, \xi),$$

we obtain

$$\begin{aligned} t \frac{\partial N_1}{\partial t} + \frac{\partial N_1}{\partial \tau} (s + v_1) + \frac{\partial v_1}{\partial \tau} (N_e + N_1) + v_1 \frac{dN_e}{d\tau} + N_1 \frac{dv_e}{d\tau} &= 0, \\ t \frac{\partial v_1}{\partial t} + \frac{\partial v_1}{\partial \tau} (s + v_1) + v_1 \frac{dv_e}{d\tau} + \frac{s^2}{N_e} \frac{\partial N_1}{\partial \tau} + N_1 \frac{d(s^2/N_e)}{dN_e} \frac{dN_e}{d\tau} \\ + \frac{Ms^4}{4\pi e^2 Z N_e^2 t^2} \frac{\partial^2 N_1}{\partial \xi^2} &= 0. \end{aligned} \quad (25)$$

We have taken here into account the relations (7) and (21).

Under the conditions (15), when the scale of the perturbations is large compared with the Debye radius and small compared with the characteristic scale of the variation of the self-similar solution, Eqs. (25) have in first-order approximation solutions of the type of simple waves

$$N_1 = N_{10}(v_1). \quad (26)$$

In this case

$$\frac{dN_{10}}{dv_1} = \frac{dN_e(\tau)}{dv_e} = \frac{N_e}{s} t \frac{\partial v_1}{\partial t} + v_1 \frac{\partial v_1}{\partial \tau} = 0, \quad (27)$$

i.e.,  $v_1$  is constant on the lines  $\tau = v_1 \ln t + C$ .

It is natural under the same conditions to seek a more general solution in a form close to a simple wave:

$$N_1 = N_1(v_1) + \delta N_1(t, \tau), \quad (28)$$

where  $\delta N_1$  is quantity of higher order of smallness. Substituting expression (28) in Eq. (25) and taking (26), (27), and (7) into account, we arrive at the following equation for  $v_1$ :

$$\frac{\partial v_1}{\partial \xi} + v_1 \frac{\partial v_1}{\partial \tau} + \alpha(\xi, \tau) \frac{\partial^2 v_1}{\partial \tau^2} + \beta(\tau) v_1 + \gamma(\tau) N_1(v_1) = 0; \quad (29)$$

$$\xi = \ln t, \quad \alpha(\xi, \tau) = \frac{Ms^4(\tau)}{8\pi e^2 Z N_e(\tau) e^{2\xi}}, \quad \beta(\tau) = \frac{dv_e}{d\tau},$$

$$\gamma(\tau) = \frac{1}{2} \left( \frac{dv_e}{d\tau} \frac{s}{N_e} + \frac{d(s^2/N_e)}{dN_e} \frac{dN_e}{d\tau} \right).$$

The calculations in the derivation of (29) are fully analogous to those usually employed to derive the Korteweg-de Vries equation (see Ref. 22, §15). Equation (29) differs from it in the last two terms, which take into account the inhomogeneity of the medium in which the perturbation propagates. In addition, in place of the time we have here  $\xi = \ln t$  and the coefficient of the higher-order derivative depends significantly on  $\xi$  and  $\tau$ . Neglecting the inhomogeneity we have

$$\frac{dv_e}{d\tau} \rightarrow 0, \quad \frac{dN_e}{d\tau} \rightarrow 0, \quad s \neq s(\tau), \quad N_e \neq N_e(\tau)$$

and over distances  $\Delta x \ll \tau t$  it goes over into the usual Korteweg-de Vries equation.

The perturbations described by Eq. (29) are close to self-similar. It is natural therefore to call them quasi-self-similar waves. The profile of quasi-self-similar waves in terms of self-similar variables, as follows from (29), varies slowly with time. Quasi-self-similar waves are always excited upon expansion of a multi-component plasma (see §3).

We have considered above one-dimensional planar motion of a plasma with an abrupt initial ion boundary (11). Numerical solutions of Eqs. (3) and (4) show that

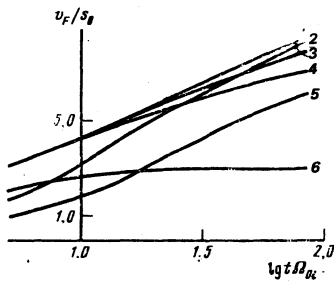


FIG. 4. Ion-front velocity  $v_F/s_0$ ,  $s_0 = (T_e/M)^{1/2}$ , as a function of the time  $t$  for a Maxwellian electron distribution function: 1) planar problem with abrupt boundary; 2) planar problem with non-abrupt boundary; 3) cylindrical problem with abrupt boundary,  $R_0 = 100D$ ; 4) cylindrical problem with abrupt boundary,  $R_0 = 10D$ ; 5) cylindrical problem with non-abrupt boundary; 6) spherical problem with abrupt boundary,  $R_0 = 10D$ ,  $D = (T_e/4\pi e^2 N_0)^{1/2}$ ,  $R_0$  is the initial radius of the cylinder or the sphere.

the acceleration retains its character also when the initial boundary is not too strongly smeared. In this case, in the region where the ion density initially vanished smoothly, there is produced an abrupt front of finite intensity, which evolves in the course of time in the same manner as in the problem with the abrupt initial boundary. The formation of this front can be easily understood if it is noted that in the region where  $N$  vanishes smoothly at  $t=0$  the electron density  $N_e$  should exceed  $N$ , and the acceleration of the ions in this region is initially smaller than that of the ions located on the left, in the region where  $N_e < N$ . As seen from Fig. 4, in the case of smeared boundary the total acceleration of the ions (at  $t\Omega_{oi} \gg 1$ ) does not differ greatly from the acceleration in the case of a sharp boundary.

Figure 4 shows also the velocity of the ion front for the expansion of plasma cylinders with abrupt and smeared boundaries. It is seen that in the cylindrical case the ion acceleration is less considerable and also preserves its character in the case of weak smearing of the initial boundary. The figure shows also the velocity of the ion front an expanding a plasma sphere with abrupt boundary. In this case  $v_F$  is bounded.<sup>23</sup>

### §3. EXPANSION OF MULTICOMPONENT PLASMA

We have assumed above that the plasma consists of one sort of ions. In real problems the plasma has frequency many components, i.e., it consists of ions with different masses  $M_k$  and charges  $Z_k$ . Equations (3) are written in this case independently for each ion component:

$$\frac{\partial N_k}{\partial t} + v_k \frac{\partial N_k}{\partial x} + N_k \frac{\partial v_k}{\partial x} = 0, \quad (30)$$

$$\frac{\partial v_k}{\partial t} + v_k \frac{\partial v_k}{\partial x} + \frac{eZ_k}{M_k} \frac{\partial \varphi}{\partial x} = 0.$$

In the Poisson Eq. (4),  $N$  is now the summary effective ion density

$$N = \sum N_k Z_k. \quad (31)$$

It is seen from (30) and (31) that in a multicomponent plasma the ion acceleration depends essentially on the ratio  $Z_k/M_k$ . For ions with the same ratio  $Z_k/M_k$ , Eqs. (30) are identical. This means that the acceleration of such ions is identical, i.e., their relative densities  $N_k/N_{k0}$  have an identical dependence on the velocity  $v_k$ . It is also obvious that ions with larger values of  $Z_k/M_k$  are more strongly accelerated.

If the plasma contains one basis ion component  $Z_1$ ,  $M_1$  and small impurities of ions  $Z_k, M_k$ , such that  $N_1 Z_1 \gg \sum_{k>1} N_k Z_k$ , then the potential  $\varphi$  is determined by the basic component. The acceleration of the different ions depends then on the parameter

$$p_k = M_1 Z_k / Z_1 M_k. \quad (32)$$

A special situation arises then for Maxwellian electrons. In this case  $\partial\varphi/\partial x = \text{const}/t$  (9) and Eqs. (31) for the different impurity components are identical in form when  $v_k$  is renormalized to  $(p_k)^{1/2}$ . This means that the energy spectra of the accelerated impurity ions should be similar, with a similarity parameter  $p_k$ .<sup>7</sup>

We consider now a plasma consisting of two components—ions  $N_1, Z_1, M_1$  and  $N_2, Z_2, M_2$ . In the self-similar limit, Eqs. (30), (31), and (5) take then the form

$$(v_1 - \tau) \frac{dN_1}{d\tau} + N_1 \frac{dv_1}{d\tau} = 0, \quad (v_2 - \tau) \frac{dN_2}{d\tau} + N_2 \frac{dv_2}{d\tau} = 0,$$

$$(v_1 - \tau) \frac{dv_1}{d\tau} + \frac{eZ_1}{M_1} \frac{d\varphi}{d\tau} = 0, \quad (v_2 - \tau) \frac{dv_2}{d\tau} + p_2 \frac{eZ_1}{M_1} \frac{d\varphi}{d\tau} = 0, \quad (33)$$

$$N_e(\varphi) = Z_1 N_1 + Z_2 N_2, \quad p_2 = Z_2 M_1 / M_2 Z_1.$$

The dependence of  $N_e$  on  $\varphi$  at an arbitrary electron distribution function is determined as before by relation (2).

The system (33) has the integral

$$\frac{1}{e} \left( \frac{dN_e}{d\varphi} \right) = \frac{Z_1^2 N_1}{M_1 (v_1 - \tau)^2} + \frac{Z_2^2 N_2}{M_2 (v_2 - \tau)^2}.$$

In the case of a Maxwellian distribution this integral coincides with the one previously obtained.<sup>7,24</sup> Using it, we eliminate from Eqs. (33) one of the variables, and we rewrite these equations in the form

$$\frac{dv_1}{d\tau} = -\frac{F}{v_1 - \tau}, \quad \frac{dv_2}{d\tau} = -\frac{F}{v_2 - \tau} + (1 - p_2^{-1/2}), \quad \frac{d\varphi}{d\tau} = \frac{M_1}{eZ_1} F,$$

$$F = 2 \left( N_e / \frac{dN_e}{d\varphi} \right)^{1/2} \frac{s_1 s_2}{s_1^2 - s_2^2} (s_1 (1 - s_2^2) - p_2^{-1/2} s_1 (1 - s_1^2)) / \left[ s_1^2 s_2^2 \frac{d^2 N_e}{d\varphi^2} / \left( \frac{dN_e}{d\varphi} \right)^2 - 3(s_1^2 + s_2^2 - 1) \right],$$

$$s_1 = (v_1 - \tau) / \left( N_e / \frac{dN_e}{d\varphi} \right)^{1/2}, \quad s_2 = (v_2 - \tau) / \left( N_e / \frac{dN_e}{d\varphi} \right)^{1/2}. \quad (34)$$

Equations (34) were integrated numerically with boundary conditions

$$v_{1-} = v_{2-} = v_p = \left( \frac{N_{10}/N_{20} + p_2}{N_{10}/N_{20} + 1} \right)^{1/2}; \quad N_{1-} = N_{10}; \quad N_{2-} = N_{20},$$

corresponding to the problem of expansion of a half-space into vacuum. The velocity  $v_p$  is the velocity of a rarefaction wave traveling in the direction of the dense plasma (see Ref. 23). The distributions of the densities  $N_1$  and  $N_2$  and of the velocities  $v_1$  and  $v_2$  are shown for the case of Maxwellian electrons in Figs. 5 and 6.

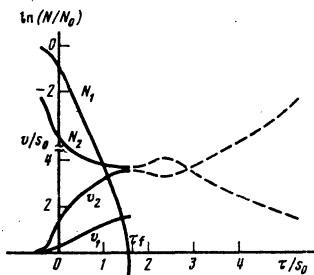


FIG. 5. Change of the density and velocity of the ions as a function of  $\tau/s_0$ ,  $s_0 = (T_e/M_2)^{1/2}$  in the case of expansion, into vacuum of a plasma containing a mixture of 90% oxygen ions  $O^+$  ( $N_1, v_1$ ) and 10% of hydrogen ions  $H^+$  ( $N_2, v_2$ ). At  $\tau = \tau_f \approx 1.7s_0$  the oxygen density vanishes. Dashed—distributions, obtained by integrating the total system of equations (30) and (31), of the density and velocity of the hydrogen past the singular point  $\tau_f$ .

It is seen that the ion motion depends significantly on the ratio  $Z_k/M_k$ . Interesting qualitative peculiarities also arise. In a one-component plasma the ion density vanishes only as  $\tau \rightarrow \infty$ , inasmuch as in the quasineutral limit (5) the potential  $\phi \rightarrow \infty$  in the place where  $N \rightarrow 0$ . In a two-component plasma the situation is different. Here the component of the ions with the smaller  $Z_k/M_k$  is less accelerated by the electric field. Their density  $N_k$  decreases more rapidly than the density of the second component. Therefore, at  $Z_1/M_1 \ll Z_2/M_2$  the density  $N_1$  becomes equal to zero at a certain finite value  $\tau = \tau_f$  (Fig. 5). The potential  $\phi$  remains, naturally, finite in this case [since the density  $N_2 \neq 0$ , and  $\phi$  is determined by the combined density (31)]. The ions of the first component are accelerated consequently only to a velocity  $v_1 = \tau_f$  and exist only at  $\tau \leq \tau_f$ . At  $\tau > \tau_f$  these ions do not exist, so that the remaining component  $Z_2, M_2$  propagates here alone. Near  $\tau_f$  there is produced in this case a region of very slow  $N_2(\tau)$  variation—a plateau region.

In the case when the difference between  $Z_1/M_1$  and  $Z_2/M_2$  is small, the density  $N_1$  does not vanish and the plateau region is not strongly pronounced: there is only a region with a slower decrease of the density  $N_2$  (the region  $\tau/s_0 \sim 1-4$  in Fig. 6).

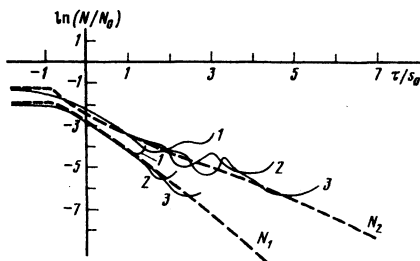


FIG. 6. Change of the ion density as a function of  $\tau/s_0$ ,  $s_0 = (T_e/M_2)^{1/2}$  in the case of expansion, in a vacuum, of a plasma containing a mixture of 1/3 carbon ions  $C^{+6}(N_1)$  and 2/3 hydrogen ions  $H^+(N_2)$ . Solid curve—solution of complete system of equations (30) and (31) at various instants of time: 1)  $t\Omega_{0i} = 15$ ; 2)  $t\Omega_{0i} = 35$ ; 3)  $t\Omega_{0i} = 65$ . Dash—self-similar solution.

Solutions with allowance for the complete Poisson Eq. (4) show, just as in a one-component plasma, a gradual transition to a regime close to self-similar. However, the presence of steep fronts of the two ion components leads to excitation of quasi-self-similar waves. They are particularly intense in the region of plateau or the slow decrease of the density  $N_2$  (Fig. 6). The region of the slow decrease turns out to be more strongly pronounced than in the self-similar regime. We note that analogous self-similar waves are excited also in the kinetics of a quasineutral plasma.<sup>7</sup>

#### § 4. ION ACCELERATION IN A LASER PLASMA

Accelerated ions are observed in an expanding laser plasma. In the case of short intense laser pulses, the rapid ions carry away up to 50% of the absorbed energy.<sup>9-11</sup> An investigation of the x rays shows that the electrons have a non-Maxwellian velocity distribution with a clearly pronounced high-energy tail.<sup>25,26</sup> Since it is precisely the energetic electrons that are important for the ion acceleration, an investigation of the fast-ion spectra can be useful for the diagnostics of a laser plasma.

We shall consider the results of Decoste and Ripin,<sup>10</sup> which are most detailed. A neodymium-laser pulse ( $\lambda = 1.06 \mu\text{m}$ ,  $\Delta t = 75 \text{ psec}$ ,  $W \approx (1-2) \times 10^{16} \text{ W/cm}^2$ ) irradiated flat targets of  $CD_2$ ,  $CH_2$ , and  $CH$ . The radius of the focal spot (at half laser power) was  $R_0 \approx 10-12 \mu\text{m}$ . In a chamber of  $\sim 75 \text{ cm}$  diameter, a vacuum  $\sim 10^{-6}-10^{-7}$  Torr was maintained, so that collisions and charge exchange could be avoided in the ion flux dispersing away from the target.

The distribution of the accelerated ions was investigated with ion analyzers. It was observed in this case that the ions were in the main completely ionized, i. e., the ions  $C^{+6}$  and the ions  $H^+$  or  $D^+$  were observed, depending on the type of target. Figures 7 and 8 show the energy distribution of the ions  $C^{+6}$ ,  $D^+$ , and  $H^+$  produced when  $Cd_2$  and  $CH_2$  targets are irradiated. It is seen that the carbon ions  $C^{+6}$ , which have the large charge  $Z = 6$ , are accelerated to high energies  $\sim 1 \text{ MeV}$ . The energy spectra contain a number of peaks whose heights and positions vary substantially from experiment to experiment. On the other hand, the (smoothed) curves

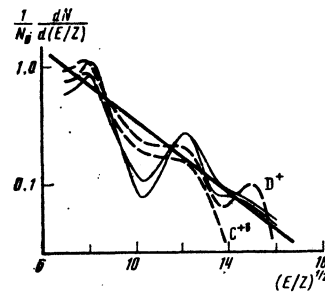


FIG. 7. Energy spectra of accelerated ions  $C^{+6}$  and  $D^+$  for a  $CD_2$  target in two different realizations.<sup>10</sup> Solid line—first experiment, dashed—second experiment. Thick solid line—calculation in accord with the theory in the self-similar approximation for  $T_e = 15 \text{ keV}$ .  $E$ —energy in keV,  $Z$ —ion charge.

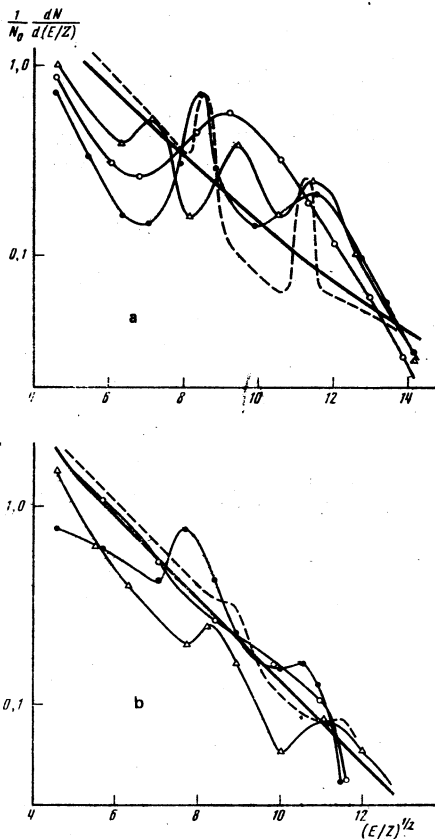


FIG. 8. Energy spectra of accelerated  $H^+$  (a) and  $C^{+6}$  (b) ions for a  $CH_2$  target in various realizations.<sup>10</sup> Thick solid lines—calculation in accord with the theory in the self-similar approximation at  $T_e = 15$  keV, dashed—solution of the complete system of equations (30) and (31) at  $t\Omega_{ci} = 50$ .  $E$  is the energy in keV and  $Z$  is the ion charge.

averaged over the oscillations are stable. We note that simultaneous measurements of the x rays in the 1–100 keV band show the distribution of the electrons in the plasma to be on the whole essentially non-Maxwellian, but in the region of the tail of the distribution function,  $20 \text{ keV} \leq \varepsilon \leq 100 \text{ keV}$ , the electron spectrum is approximately Maxwellian with an effective electron temperature

$$T_e \approx 15-18 \text{ keV.} \quad (35)$$

We compare now the results of the experiments with the theory.

**Dependence on  $Z/M$ .** It is seen from Fig. 7 that in terms of the chosen variables the energy spectra of the ions  $C^{+6}$  and  $D^+$ , which are produced by irradiation of  $CD_2$  targets, are the same in each realization—they practically coincide. This is in full agreement with the theory considered here. Indeed, the ions  $C^{+6}$  and  $D^+$  have the same  $Z/M$  ratio. Equations (30) for them are identical, and in this case, as indicated in §3, the relative densities of the accelerated ions  $N_k/N_{k0}$  should have the same dependence on their velocity  $v_k = (E/Z)^{1/2}(2Z/M)^{1/2}$ . This is well confirmed by the experimental data. On the contrary, for  $C^{+6}$  and  $H^+$ , which have different  $Z/M$  ratios, the experimental spectra are substantially different (Fig. 8), as they should.

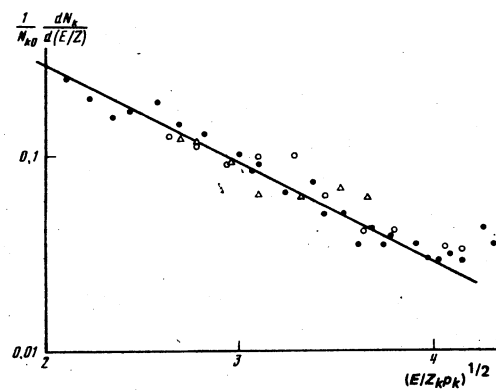


FIG. 9. Spectra of the ions  $O^{+8}$ ,  $C^{+6}$  ( $\bullet$ ),  $C^{+5}$  ( $\circ$ ), and  $O^{+7}$  ( $\Delta$ ) (Ref. 11) as functions of the parameter  $(E/Z_k p_k)^{1/2}$ ;  $E$ —energy in keV,  $Z_k$ —charge of ions,  $p_k$ —similarity parameter (32). Relative ion concentrations  $N_0 O^{+8}$ ,  $C^{+6}$ :  $N_0 C^{+5}$ :  $N_0 O^{+7} = 1:0.8:0.4$ . Solid line—theory [(9) and (32)].

**Averaged spectra.** The thick solid curves in Figs. 7 and 8 are the results of the calculation of the energy spectra of the ions in the self-similar approximation.<sup>5)</sup> One can see sufficient agreement with the averaged experimental data. The electron temperature was assumed in the calculation to be 15 keV, in agreement with (35). We note that the averaged energy spectrum of the ions on Figs. 7, when plotted in logarithmic scale, decreases linearly with increasing ion velocity, in accordance with the predictions of the theory.<sup>1</sup> The same dependence is clearly seen also in Fig. 9, which shows the spectra of various impurity ions, obtained by Berger *et al.*,<sup>11</sup> and renormalized to a unified theoretical curve. Here, too, the similarity law of the impurity-ion spectra is well satisfied with a similarity parameter (32).

In the case shown in Fig. 8, ions with different  $Z/M$  are accelerated. The region of the slow decrease (plateau) of the  $A^+$  ions is clearly seen on the experimental curves, in agreement with the calculation (see Fig. 6).

**Oscillations of the spectrum.** The oscillations of the energy spectrum can be naturally connected with the excitation of quasi-self-similar waves. As seen from (36), in the self-similar limit an important role is played not only by the  $N(\tau)$  oscillations, but also by the  $dv/d\tau$  oscillations which can lead to an enhancement of the spectrum oscillations. According to the numerical calculation data (Fig. 6), the characteristic period of the oscillations is

$$\Delta v \approx 1-1.2(T_e/M_n)^{1/2}. \quad (37)$$

It is seen from the experimental curves of Fig. 7 and 8 that the period is

$$\Delta(E/Z)^{1/2} \approx 2.2-3 \text{ keV.} \quad (38)$$

From a comparison of (37) and (38) it follows that  $T_e \approx 10-20$  keV, in rough agreement with (35).

**Energy limits of accelerated ions.** The maximum ion-acceleration energy is strongly influenced by the dimension of the focal spot on the target, which deter-

mines the size of the produced plasma. According to (20), the maximum ion energy is given by

$$\left(\frac{E}{Z}\right)_M = \frac{M}{2Z} v_M^2 = 2T_e [\ln^2(t_M \Omega_0)], \quad \Omega_0 = \left(\frac{4\pi e^2 N_0}{M}\right)^{1/2}. \quad (39)$$

Here  $t_M$  is the total acceleration time.

Recognizing that the acceleration takes place only up to a certain distance  $R_M$  from the target, we find that the time  $t_M$  is given by

$$y_M \ln y_M \approx \frac{R_M}{D} \frac{1}{2Z^{3/2}}, \quad D = \left(\frac{T_h}{4\pi e^2 N}\right)^{1/2}, \quad y_M = t_M \Omega_0, \quad (40)$$

where  $D$  is the Debye radius for the fast electrons. Recognizing that on the plasma boundary (i.e., at the point of reflection of the laser wave) the electron density is

$$N_0 = m\omega_p^2/4\pi e^2, \quad \omega_p = 2\pi c/\lambda, \quad (41)$$

we obtain  $y_M \approx 20$  for a  $\text{CD}_2$  target. We have taken into account here the fact that the average charge in the  $\text{C}^{+6} + 2\text{D}^+$  mixture is  $Z = 8/3$ , and set the distance  $R_M$  equal to the radius  $R_0$  of the focal spot. At distances larger than  $R_0$ , the plasma expansion is no longer one-dimensional, and the ion acceleration in the direction normal to the target is practically stopped.<sup>21,23</sup> We then get from (39) for  $\text{C}^{+6}$  ions at  $T_e = 16\text{--}18$  keV an energy limit  $(E/C)_M \approx 250\text{--}280$  keV, in agreement with the experimental data.<sup>10</sup> For the  $\text{D}^+$  ions, allowance must be made for the fact that deuterium can begin to expand freely before the  $\text{C}^{+6}$  ions (by virtue, e.g., of the faster ionization). Consequently, the limiting energies of the deuterium ions are determined by the expansion of the  $\text{D}^+$  plasma with  $Z = 1$ . According to (39) and (40), at the same value of  $R_M$  we obtain  $y_M \approx 30$  and  $(E/Z)_M \approx 350$  keV, in accord with the experimental data.

For  $\text{CH}_2$  targets, the limiting energies of the  $\text{H}^+$  ions are approximately the same as for the  $\text{D}^+$  ions, and the limiting energies of the  $\text{C}^{+6}$  ions are somewhat lower:  $(E/Z)_M \approx 180$  keV, since the  $\text{C}^{+6}$  ions in the mixture with  $\text{H}^+$  are less accelerated because of the lower value of  $Z/M$  (see Fig. 5).

**One-dimensional character of the acceleration.** In the experiments represented in Fig. 7 and 8, the accelerated ions were observed in a direction normal to the target. Decoste and Ripin<sup>10</sup> report also results of measurements at a small angle  $\alpha = 12.5^\circ$  to the normal ( $\text{CH}_2$  target). The distribution of the  $\text{C}^{+6}$  ions is then substantially changed—the number of fast ions is much less than in the case of propagation in the normal direction. This shows that the ions are accelerated mainly in a direction normal to the plate, and consequently the ion acceleration is one-dimensional in accord with the theory considered here. That the ion acceleration in short-laser pulses is one-dimensional is indicated also by the experiments of Ref. 9.

We emphasize that to describe the motion of the ions in the theory presented here we have used the equations of ideal hydrodynamics in a strong electric field (3), which are valid at arbitrary ion mean free paths. For impurity ions with  $Z/M$  different from that of the main ions, the collisions may turn out to be substantial, and

if they play the decisive role, Eq. (3) is again valid, with  $Z$  and  $M$  representing the average mass and the average charge of the ions. On the other hand, the electron motion is assumed to be collisionless [Eqs. (1) and (2)]. We estimate therefore the electron mean free path  $l_e$ . In the region near the start of the expansion we have  $l_e \approx 18 \text{ e}^2 \mu\text{m}$ ; the electron energy  $\varepsilon$  is expressed here in keV, and account is taken of the fact that for a neodymium laser the electron density calculated from (41) is  $N_0 \approx 10^{21} \text{ cm}^{-3}$ . It is seen therefore that for electrons with energy  $\varepsilon \geq 3$  keV the condition of collisionless expansion  $l_e \gg R_0$  is well satisfied.

We note in conclusion that our analysis can explain the mechanism of effective transfer of energy of an intense laser pulse to the dispersing accelerating ions. When a laser pulse acts on a target, the resultant plasma is pushed towards the target by the pressure of the light. The electrons are reflected from the inhomogeneous alternating electric field of the wave, which produces in fact the barrier  $\varepsilon_M$  that contains the plasma. This persists, however, only to electrons whose kinetic energy is  $\varepsilon \leq \varepsilon_M = e^2 E_M^2 / 4m\omega^2$ ; here  $E_M$  is the maximum amplitude of the wave field. The energy  $\varepsilon_M$  is several times larger than the thermal energy of the plasma electron in the region of wave reflection. The fast electrons, whose energy exceeds  $\varepsilon_M$ , are not retained by the electromagnetic barrier. At  $\varepsilon \gg \varepsilon_M$  the barrier is of no effect at all—these electrons expand freely in the vacuum. It is they which lead to the ion acceleration observed in the experiment. For example, in the previously considered experiments of Ref. 10, the average thermal energy of the electrons was of the order of 1 keV, and the height of the barrier was  $\varepsilon_M \sim (5\text{--}15)$  keV, whereas the observed ion acceleration was effected by electrons with energies 20–200 keV.

It is important that with increasing laser-pulse energy a larger role is assumed by the anomalous mechanism of absorption of its energies,<sup>27</sup> which leads to the appearance of a large number of fast electrons. These electrons are not retained by the field of the wave. When the plasma spreads they give up their energy to the accelerated ions. It is this which causes the very effective transfer of the anomalously absorbed energy of the intense laser pulse to the energy of the expanding fast ions.

The authors thank L. P. Pitaevskii for a helpful discussion.

1) Accelerated ions are also observed in laser pulses of lower intensity and longer duration, although they seem to play a lesser role.<sup>12</sup>

2) If the potential has a nonmonotonic variation it is necessary to use an adiabatic distribution of the electrons.<sup>13,14</sup>

3) The influence of hydrodynamic motion on the electron distribution was taken into account by Denavit<sup>15</sup> and by Mora and Pellat.<sup>16</sup>

4) The power-low dependence chosen by us,  $N_e(\varphi) \sim (1 - e\varphi/T_e)^{-2}$  corresponds to an electron distribution function

$$f_e(v_e) = \frac{3N_0}{4v_T} \left[ 1 + \left(\frac{v}{v_T}\right)^2 \right]^{-3/2}, \quad v_T = \left(\frac{2T_e}{m}\right)^{1/2}.$$

5) The energy distribution of the accelerated ions observed at

the point  $x_0$  is very simply connected with  $N(\tau)$  and  $v(\tau)$ .<sup>7,18</sup> Let  $\pi$  be the total number of ions passing through a unit area at the point  $x_0$ :  $\pi = \int Nvdt$ . Then

$$\frac{1}{N_0} \frac{d\pi}{d(E/Z)} = \frac{M}{Z} \frac{x_0}{N_0} N(\tau) \left/ \left( v \frac{dv}{d\tau} \right)_{\tau} \right.,$$

where the function  $\tau(E)$  is defined in accordance with  $\tau = \tau(v)$ ,  $v = (2E/M)^{1/2}$  [see (8a)]. From (36) it is seen that the energy spectrum in its basic exponential part is determined by the course of the  $N(\tau)$  dependence.

<sup>1</sup>A. V. Gurevich, L. V. Pariiskaya, and L. P. Pitaevskii, Zh. Eksp. Teor. Fiz. **49**, 647 (1965) [Sov. Phys. JETP **22**, 449 (1966)].

<sup>2</sup>A. A. Plyutto, V. N. Ryshkov and A. T. Kalin, *ibid.* **47**, 494 (1964) [20, 328 (1965)].

<sup>3</sup>P. Kórn, T. C. Marshall, and S. P. Schlesinger, Phys. Fluids **13**, 517 (1970).

<sup>4</sup>G. C. Goldenbaum and K. A. Gerber, *ibid.* **16**, 1269 (1972).

<sup>5</sup>V. G. Eseevich and V. G. Fainshtein, Dokl. Akad. Nauk SSSR **244**, 1111 (1979) [Sov. Phys. Dokl. **24**, 114 (1979)].

<sup>6</sup>U. Samir and G. L. Wrenn, Planet. Space Sci. **17**, 693 (1969).

<sup>7</sup>A. V. Gurevich, L. V. Pariiskaya and L. P. Pitaevskii, Zh. Eksp. Teor. Fiz. **63**, 516 (1972) [Sov. Phys. JETP **36**, 274 (1977)].

<sup>8</sup>Yu. A. Zakharenkov, O. N. Krokhin, G. V. Sklizkov, and A. S. Shikanov, Pis'ma Zh. Eksp. Teor. Fiz. **25**, 415 (1977) [JETP Lett. **25**, 388 (1977)].

<sup>9</sup>P. Wägli and T. P. Donaldson, Phys. Rev. Lett. **40**, 875 (1978).

<sup>10</sup>R. Decoste and B. M. Ripin, *ibid.* **40**, 34 (1978). R. Decoste, NRL Report 3774, Washington, 1978.

<sup>11</sup>R. L. Berger *et al.*, Proc. 7th Int. Conf. on Plasma Phys. and Contr. Nucl. Fusion, Innsbruck, 1978.

<sup>12</sup>N. E. Andreev, Yu. A. Zakharenkov, N. N. Zorev, V. T. Tikhonchuk, and A. S. Shikanov, Zh. Eksp. Teor. Fiz. **76**, 953 (1979) [Sov. Phys. JETP **49**, 492 (1979)].

<sup>13</sup>A. V. Gurevich, *ibid.* **53**, 953 (1967) [26, 575 (1968)].

<sup>14</sup>E. M. Lifshitz and L. P. Pitaevskii, Fizicheskaya kinetika (Physical Kinetics), Nauka, 1979, §36.

<sup>15</sup>J. Denavit, Phys. Fluids **22**, 1384 (1979).

<sup>16</sup>P. More and R. Pellat, *ibid.* p. 2300.

<sup>17</sup>S. I. Anisimov and Yu. V. Medvedev, Zh. Eksp. Teor. Fiz. **76**, 121 (1979) [Sov. Phys. JETP **49**, 62 (1979)].

<sup>18</sup>L. M. Wickens, J. E. Allen, and P. R. Rumsby, Phys. Rev. Lett. **41**, 243 (1978).

<sup>19</sup>A. Gurevich, D. Anderson, and H. Wilhelmsson, *ibid.* **42**, 769 (1979).

<sup>20</sup>B. Bezzirides, D. W. Forslund, and E. L. Lindeman, Phys. Fluids **21**, 2179 (1978).

<sup>21</sup>A. V. Gurevich and L. P. Pitaevskii, in: Voprosy teorii plazmy (Problems of Plasma Theory), M. A. Leontovich, ed., No. 10, Atomizdat, 1980, §3.